Theoretical Kinetics of O + C_2H_4

Xiaohu Li,[1] Ahren W. Jasper,[1] Judit Zádor,[1] James A. Miller,[2] and Stephen J. Klippenstein[2]

[1]*Combustion Research Facility, Sandia National Laboratories, Livermore, CA 94551, USA*
[2]*Chemical Sciences and Engineering Division, Argonne National Laboratory, Argonne, IL 60439, USA*

Corresponding author: Ahren Jasper, email: ajasper@sandia.gov
Sandia National Laboratories
PO Box 969
Livermore, CA 94550-0969 USA

Colloquium: Reaction Kinetics

Word Count (Method 1):

Abstract	262
Main Text	4360
References	682
Equations	167
Figure 1	220
Figure 2	141
Figure 3	145
Figure 4	153
Figure Captions	193
Table 1	122
Total (excl. abstract)	**6183**

Theoretical Kinetics of O + C_2H_4

Xiaohu Li,[1] Ahren W. Jasper,[1] Judit Zádor,[1] James A. Miller,[2] and Stephen J. Klippenstein[2]

[1]*Combustion Research Facility, Sandia National Laboratories, Livermore, CA 94551, USA*
[2]*Chemical Sciences and Engineering Division, Argonne National Laboratory, Argonne, IL 60439, USA*

Abstract

The reaction of atomic oxygen with ethylene is a fundamental oxidation step in combustion and is prototypical of reactions in which oxygen adds to double bonds. For $^3O+C_2H_4$ and for this class of reactions generally, decomposition of the initial adduct via spin-allowed reaction channels on the triplet surface competes with intersystem crossing (ISC) and a set of spin-forbidden reaction channels on the ground-state singlet surface. The two surfaces share some bimolecular products but feature different intermediates, pathways, and transition states. The overall product branching is therefore a sensitive function of the ISC rate. The $^3O+C_2H_4$ reaction has been extensively studied, but previous experimental work has not provided detailed branching information at elevated temperatures, while previous theoretical studies have employed empirical treatments of ISC. Here we predict the kinetics of $^3O+C_2H_4$ using an ab initio transition state theory based master equation (AITSTME) approach that includes an a priori description of ISC. Specifically, the ISC rate is calculated using Landau-Zener statistical theory, consideration of the four lowest-energy electronic states, and a direct classical trajectory study of the product branching immediately after ISC. The present theoretical results are largely in good agreement with existing low-temperature experimental kinetics and molecular beam studies. Good agreement is also found with past theoretical work, with the notable exception of the predicted product branching at elevated temperatures. Above ~1000 K, we predict CH_2CHO+H and CH_2+CH_2O as the major products, which differs from the room temperature preference for CH_3+HCO (which is assumed to remain at higher temperatures in some models) and from the prediction of a previous detailed master equation study.

Keywords: Cvetanović, non-adiabatic transition state theory, RRKM

1. Introduction

Historically, the two most significant nonadiabatic reactions in combustion have been the reaction of CH with N_2 and the reaction of ^3O with C_2H_4. The first of these reactions is responsible for Fenimore's prompt NO [1]. Until relatively recently this reaction was thought to start out on a doublet surface, undergo an intersystem crossing (ISC) to a quartet surface, and end up producing HCN+^4N as the primary products [2,3]. We now believe with some certainty that this channel is a minor one, and that the main channel is an adiabatic process producing NCN+H [4,5].

The situation is not so clear for $^3O+C_2H_4$. This long-studied reaction (with significant contributions from Cvetanović [6]) takes place by first forming a weakly bound complex on a triplet surface. This complex can rearrange or dissociate to form several sets of products. It can also change its electron spin and transition nonadiabatically to the singlet surface, where it can undergo a completely different set of rearrangements and dissociations. A variety of bimolecular product channels have been identified and proposed.

$^3O + C_2H_4$	$\rightarrow$	$CH_3 + HCO$	(1a)
	$\rightarrow$	$CH_3CO + H$	(1b)
	$\rightarrow$	$CH_2CHO + H$	(1c)
	$\rightarrow$	$C_2H_3 + OH$	(1d)
	$\rightarrow$	$^3CH_2 + CH_2O$	(1e)
	$\rightarrow$	$^1CH_2 + CH_2O$	(1e')
	$\rightarrow$	$CH_2CO + H_2$	(1f)
	$\rightarrow$	$CH_4 + CO$	(1g)
	$\rightarrow$	$C_2H_2 + H_2O$	(1h)

While the total rate coefficient for reaction 1 appears to be reasonably well established experimentally over a wide range of temperatures, the product distribution is not. The most recent Baulch et al. [7] compilation recommends the following product distribution at room temperature and <1 bar: 60% CH_3+HCO (1a), 35% CH_2CHO+H (1c), with minor contributions from CH_2CO+H_2 (1f) and CH_2+CH_2O (1e). All product measurements (upon which the Baulch recommendation is based) have been made at low temperatures. Theoretical analysis has shown that CH_3+HCO (1a) must come from the

singlet surface, whereas CH_2CHO+H (1c) comes from the triplet. Consequently, the rate of intersystem crossing in this system must be significant, unlike the situation for the CH+N_2 reaction.

The recommended room temperature branching fractions are in agreement with the subsequent study of Miyoshi et al. [8], who notably also addressed a potential source of disagreement in some previously reported branching fractions. Miyoshi et al. measured both CH_3 and HCO and found that [HCO]/[CH_3] varied from 0.6–0.9 for pressures from 1–4 Torr, suggesting that some fraction of HCO is formed hot and may decompose before it can be detected.

Experimental information regarding temperature-dependent branching is relatively sparse, with two experimental studies reporting only small changes with temperature up to 770 K [9] and 600 K [10,11]. The total rate coefficient and branching are expected to be largely independent of pressure, although the stabilization of oxirane and acetaldehyde/vinyl alcohol has been observed experimentally at high pressures and 300 K [12].

Reaction 1 was also studied under collisionless conditions using crossed molecular beams (see, e.g., Refs. [13-17]). In addition to the major and minor product channels mentioned above, crossed molecular beam studies have found minor contributions from CH_3CO+H (1b).

Theoretical studies of reaction 1 include the comprehensive and detailed master equation (ME) study of Nguyen et al. [11]. Their results were found to be in good agreement with the total experimental rate coefficient, the low-temperature experimental branching fractions, and the molecular beam studies summarized above. This good agreement is due in part to their empirical tuning of the relative total singlet and triplet branching fractions. Specifically, they performed separate ME calculations for the singlet and triplet channels and combined the results assuming temperature-independent weights of 55 and 45% for the singlet and triplet channels, respectively, as inferred from the low temperature experiments discussed above.

Multistate (surface hopping [18,19]) trajectory studies have also been carried out [20], including recent detailed comparisons with the experimental crossed beam studies mentioned above [15,17].

Again, the theoretical and experimental results were found to be largely in good agreement with one another. Notably, the results of Hu et al. [20] indicated some decrease in the relative importance of ISC with increasing energy, apparently in disagreement with the assumption made by Nguyen et al. Trajectory studies have the advantage that they naturally include any potential nonstatistical effects, such as those that may arise immediately following ISC noted above. The reliance on classical mechanics, however, may introduce errors, particularly at low energies. Furthermore, the trajectory studies explicitly considered only two of the four lowest-energy electronic states. The spin–orbit coupling parameter used in both sets of studies was inferred by Hu et al. in part by considering three different values and comparing with experimental branching fractions [20].

Here we use an ab initio transition state theory based master equation (AITSTME) approach, including a nonadiabatic statistical theory to describe ISC, to characterize the thermal kinetics of reaction 1 in detail. The present calculations share similarities with the ME study of Nguyen et al. [11], although somewhat different theoretical approaches have been used. The most notable differences in the two calculations relate to the treatment of ISC. Here, we have predicted the ISC rate coefficient using a Landau–Zener-based statistical theory (which is sometimes called nonadiabatic transition state theory). Direct classical trajectories calculations have also been performed to inform the ME about the (potentially nonstatistical) branching immediately following ISC to the singlet surface.

Reaction 1 is a fundamental step in hydrocarbon oxidation and generally appears in detailed chemical models of combustion. We highlight one recent study by Petersen, Curran, and co-workers [21] where sensitivity to reaction 1 was identified when modeling the oxidation of ethylene at 1000–1400 K. They noted that they could not reproduce the results of an accompanying experimental study [22] using either the room temperature branching fractions of Baulch et al. or those of Nguyen et al. The absence of experimental or a priori theoretical branching information at elevated temperatures may limit the usefulness of existing characterizations at the conditions of the Peterson, Curran, and co-workers study.

The principal goals of this work are to (1) validate the present a priori approach for predicting ISC in the context of the AITSTME approach, and (2) provide a complete set of branching fractions, including temperatures relevant to combustion. At low temperature, the present results are found to agree well with the earlier theoretical studies, including the previous ME study of Nguyen et al. [11]. At higher temperatures (above ~1000 K), however, the present study predicts CH_2CHO+H (1c) and CH_2+CH_2O (1e) as the major products, whereas the study of Nguyen et al. predicts CH_3+HCO (1a) as the dominant channel, with non-negligible contributions from CH_2CHO+H (1c) and CH_2+CH_2O (1e). These differences may be attributed to the treatment of ISC.

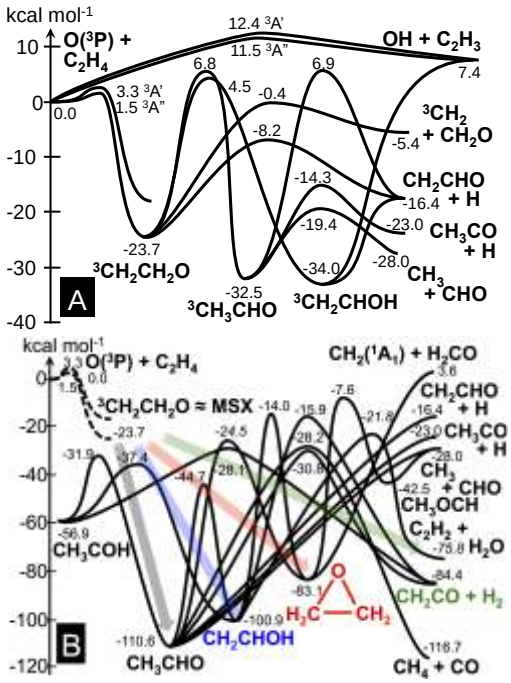

Figure 1: Potential energy diagram for the (A) triplet and (B) singlet channels. The MSX promoting ISC is close to the triplet biradical $^3CH_2CH_2O$, and the immediate products formed after ISC are indicated by arrows in B.

2. Theory

Detailed explorations of the singlet and triplet C_2H_4O potential energy surfaces (PES) have been given previously (see Refs. [11,15,20,23] and the discussions therein), and a new set of calculations was

carried out here. The resulting energies are shown in Fig. 1, where we have largely followed the scheme of Nguyen et al. [11]. The energies were calculated using a dual level approach, as detailed next. Rovibrational properties were calculated using CCSD(T)/cc-pVTZ. Energies at the CCSD(T)/cc-pVTZ geometries were obtained that include several high-level (HL) corrections: (i) CCSD(T) complete basis set (CBS) extrapolations employing the aug'-cc-pVQZ and aug'-cc-pV5Z basis sets, (ii) higher-order correlation corrections from CCSDT(Q)/cc-pVDZ calculations, (iii) core-valence corrections from CCSD(T,full)/CBS calculations based on extrapolating cc-pcVTZ and cc-pcVQZ results, (iv) relativistic corrections from CI/aug-cc-pcVTZ calculations, and (vi) anharmonic zero-point energy (ZPE) corrections calculated at the B3LYP/cc-pVTZ level. The CBS extrapolations used a two-point $l/(l+1)^4$ formula [24], Dunning correlation-consistent basis sets [25] were employed throughout, and the prime notation indicates that diffuse functions are included for only the *s* and *p* orbitals on C and N and only the *s* for H. The CCSD(T) calculations generally employed RHF wavefunctions within the UCCSD(T) formalism. The CCSDT(Q) calculations employed UHF wavefunctions, as required by Kállay's MRCC code [26]. An unpublished extensive comparison of closely related HL calculations with Active ThermoChemical Tables values indicated 2σ uncertainties in this approach of only 0.2–0.3 kcal/mol [27].

The spin-allowed fluxes associated with the transition states connecting the wells and bimolecular channels shown in Fig. 1 were calculated using several different methods, as appropriate for the different types of processes. A number of the dissociation channels produce two radicals, and the corresponding reverse reactions are barrierless. For these channels, we first used phase space theory analyses to calculate these fluxes and thereby determined that only the barrierless channels producing CH_3+HCO and CH_3CO+H from singlet CH_3CHO and producing CH_3CO+H from singlet CH_3COH contributed significantly to the kinetics. For these three channels we performed variable reaction coordinate transition state theory analyses [28]. For $[CH_3CHO \leftrightarrows CH_3+HCO]^{\ddagger}$ ($[A \leftrightarrows B]^{\ddagger}$ denotes the transition state connecting the species or bimolecular pairs A and B), we employed the methodology

described in Ref. [29], where this same process was previously considered in a different context. For [$CH_3CHO \leftrightarrows CH_3CO+H$]‡ and [$CH_3COH \leftrightarrows CH_3CO+H$]‡, we employed CASPT2(2e,2o)/cc-pVTZ direct sampling and one-dimensional corrections for geometry relaxation and basis set limitations in the VRC-TST calculations. The latter was obtained using the cc-pVQZ and cc-pV5Z basis sets.

For processes with barriers, transition state theory calculations were performed. Variational effects (at the microcanonical level) were included when calculating the kinetics for the initial addition step [$O+C_2H_4 \leftrightarrows {}^3CH_2CH_2O$]‡, as well as [${}^3CH_2CH_2O \leftrightarrows CH_2CHO+H$]‡ and [${}^3CH_2CH_2O \leftrightarrows {}^3CH_2+CH_2O$]‡. Although these processes have modest barriers in both directions, they are central to the kinetics and minor variational effects may be of some significance. Variational effects were treated using a dual level approach, CCSD(T)/CBS//B2PLYPD3/cc-pVTZ, where B2PLYPD3/cc-pVTZ was found to provide stationary point geometries and vibrational frequencies very similar to those for CCSD(T)/cc-pVTZ. Hindered rotor treatments for CH_3 and OH internal rotations were included as appropriate.

The singlet and triplet channels shown in Fig. 1 were combined in a single ME calculation, with the two networks of spin-allowed processes connected via ISC. The total ISC rate was calculated using Landau-Zener statistical theory, which is sometimes called non-adiabatic transition state theory [30,31]. In this approach, the minimum energy point on the seam of crossings (MSX, sometimes called the minimum energy crossing point or MECP) is treated as an analog of a saddle point, and equations similar to those derived for conventional (i.e., adiabatic) transition state theory are used. Here we closely follow procedures recently reviewed by Harvey [31]. In his review, he quoted this method as having an a priori error of up to an order of magnitude. When errors associated with the potential energy surfaces are minimized, however, the a priori accuracy of the method can be closer to a factor of two [32]. The "double passage" Landau–Zener formula was used here, with molecular parameters at the MSX calculated using CCSD(T)/cc-pVTZ for the crossing seam formed by the lowest-energy singlet (S_0) and

lowest-energy triplet (T_0). For weakly coupled systems such as the present one, this model correctly incorporates the fact that the ISC rate is proportional to the square of the spin–orbit coupling, ε^2.

As has been noted previously [15,20], ISC for this system occurs close to the triplet biradical, where the *two* lowest-energy singlets (S_0 and S_1) and *two* lowest-energy triplets (T_0 and T_1) all have similar energies to one another. One may evaluate the spin–orbit coupling for each of the four pairs of singlets and triplets, as was done in [20] to arrive at a total spin–orbit coupling of 70 cm^{-1}. An accompanying sensitivity test optimized this value down to between 30 and 50 cm^{-1} by comparing the results of trajectory surface hopping calculations with experimental product branching. Later trajectory studies used 35 cm^{-1} to successfully reproduce the results of molecular beam experiments [16,17].

Here we provide a different derivation but arrive at a similar value. Using multistate perturbation theory [33] (QD-NEVPT2/aug-cc-pVTZ), the MSXs for each of the S_0/T_0, S_0/T_1, and S_1/T_1 crossing seams were calculated and found to have zero-point-inclusive relative energies of ΔE_α = 0.0, 3.8, and 3.4 kcal/mol, respectively, where α labels the three seams. The MSX for S_1/T_0 could not be located, as these two states do not cross near the triplet adduct. The spin–orbit couplings for each of the three identified seams (calculated using the Breit–Pauli operator, CASSCF/aug-cc-pVTZ wavefunctions, and the ORCA software [34]) were ε_α = 19, 6.7, and 30 cm^{-1} for S_0/T_0, S_0/T_1, and S_1/T_1, respectively. We then defined an effective *total* spin–orbit coupling

$$\varepsilon_{\text{eff}}^2 = \sum_\alpha \frac{\rho_\alpha(E_{\text{ref}} + \Delta E_\alpha)}{\rho_{S_0/T_0}(E_{\text{ref}})} \varepsilon_\alpha^2 , \tag{2}$$

where ρ_{S_0/T_0} is the density of states of the MSX for S_0/T_0 evaluated at a reference energy E_{ref} (the energy of the $O+C_2H_4$ asymptote), ρ_α is the density of states of the MSX for α evaluated at an energy offset by ΔE_α, and the ratio of ρ incorporates the effects of the different thresholds for the three seams. Our resulting value (29 cm^{-1}) is close to the optimized values employed in earlier surface hopping studies [16,17,20]. The determination of ε_{eff} is potentially a significant source of a priori uncertainty in the

present calculation. The sensitivity of this parameter on the predicted product branching is discussed below.

In the ME calculation, ISC connects the initial triplet adduct to several singlet species. One could treat the MSX like a saddle point and connect the triplet adduct to whichever singlet species was found via a steepest descent path from the MSX. We found that this procedure led to either oxirane or CH_3CHO, depending on the level of ab initio theory used. The ambiguity associated with the level of theory aside, this procedure is perhaps not well justified, as, unlike saddle points, MSXs are not associated with a dynamical bottleneck in the nuclear flux. It may be more appropriate then to model ISC as depositing the system on the singlet surface at the geometries associated with the crossing seam and with large internal energies relative to nearby transition states. One may then anticipate nonstatistical "prompt" branching in the dynamics immediately following ISC.

Here we predicted this prompt branching using direct classical trajectories and the CASPT2(2e,2o)/cc-pVDZ surface. This level of theory is not quantitative globally but does give reasonable relative energies near the MSX. Each trajectory in the ensemble was initiated at the MSX (i.e., branching was assumed to be independent of the location on the seam) with a given internal energy including zero-point energy, randomized velocities, and zero total angular momentum. Ensembles consisted of 320 trajectories for each internal energy. The geometry was monitored along each trajectory, and the first identifiable "prompt product" species was determined, i.e., trajectories were not allowed to pass through multiple species. Identifiable species were formed very quickly (typically within 50 fs), supporting the present consideration of nonstatistical effects. Four channels were identified—CH_3CHO, CH_2CHOH, and oxirane as major products, and CH_2CO+H_2 as a minor product. The resulting prompt branching fractions were used to weight the total ISC rate in the ME, with the weighted ISC fluxes connecting the triplet biradical to each of the four singlet channels. Subsequent branching and the eventual formation of bimolecular products were treated as usual within the context of the ME.

Pressure dependence in the product branching fractions and the potential formation of stabilized products were considered in the master equation using estimated collision parameters. Our results were found to be independent of pressure up to fairly high pressures, with <10% variations in the branching fractions up to 20 bar at 300 K and up to 200 bar at 1000 K. These results are consistent with past experimental work at room temperature, where stabilization channels were observed from 5–70 bar [12]. We do not consider the effect of pressure further. The results presented should be suitable for most conditions relevant to combustion.

The present ME calculations were carried out using the Master Equation System Solver (MESS) program [35], which employs the chemically significant eigenvalue method for calculating rate coefficients for multiwell and multichannel systems [36].

3. Results and Discussion

The present total rate coefficient is ~30% smaller than the recommended value of Baulch et al. [7] with a somewhat larger error (50%) at 300 K; it is up to 60% smaller than the previous theoretical result of Nguyen et al. [11]. This rate is determined entirely by the two entrance barriers on the A" and A' triplet surfaces, and differences in the two theoretical results are explained by noting that the present barriers are 0.1 and 0.7 kcal/mol larger, respectively, than those employed in Ref. [11]. The experimental recommendation was assigned an uncertainty of only 10%, which is less than the expected a priori accuracy of either calculation. We therefore adjusted the properties of the transition state slightly to reproduce the recommended value.

This small adjustment (and the entrance rate in general) does not affect subsequent product branching. Instead, product branching is controlled by the fate of the initial triplet adduct $^3CH_2CH_2O$, where the ISC rate coefficient (enabling access to product channels on the singlet surface) competes with fragmentation and isomerization on the triplet surface. Unimolecular transition state theory rate coefficients for $^3CH_2CH_2O \rightarrow$ products are shown in Fig. 2, where the total rate coefficient for the

singlet product channels corresponds to the ISC rate predicted using Landau–Zener statistical theory. This value (~1.7 x 10^{11} s^{-1}) is in remarkably good agreement with the empirically inferred value of Nguyen et al. of 1.5 x 10^{11} s^{-1} [11].

Nguyen et al. made an additional assumption that the ratio of singlet products to triplet products was independent of temperature, and they used the room temperature experimental ratio of 55:45 to scale their results, even at temperatures as high at 2000 K. Figure 2 confirms that, at low energies relevant to room temperature, the total rate coefficients for forming singlet and triplet products are similar to one another. The ISC rate coefficient, however, is found here to be nearly independent of energy (and therefore temperature) whereas the triplet rate coefficients increase rapidly with energy. The almost negligible dependence of the ISC rate coefficient on energy is perhaps a bit surprising and is due in part to the similar energies and frequencies of the MSX and $^3CH_2CH_2O$. The increase in the rate coefficient with energy for the triplet channels is less surprising. As shown in Fig. 2, we can then anticipate decreased importance of the singlet product channels at elevated temperatures, in contrast to the assumption made in Ref. [11].

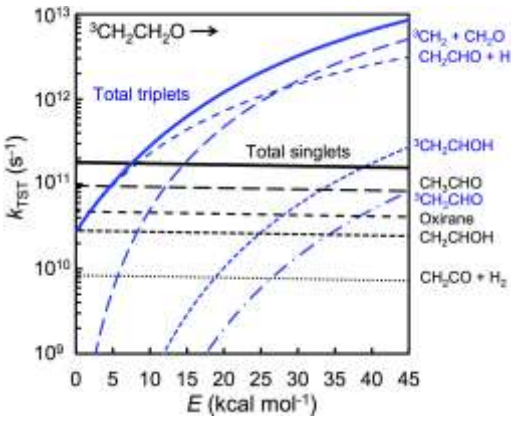

Figure 2: Unimolecular transition state theory rate coefficients (k_{TST}) for the fate of the triplet adduct $^3CH_2CH_2O$. The zero of energy is the $O+C_2H_4$ asymptote.

Figure 2 also shows that the major pathways on the triplet surface are the bimolecular channels CH_2+CH_2O (1e) and CH_2CHO+H (1c) with negligible contributions from other channels. Branching on the singlet surface is more complex. As indicated in Fig. 2, the total ISC rate coefficient was partitioned among four channels. This partitioning was determined from direct trajectory calculations, as described in Sec. 2. The results of these calculations are given in Fig. 3, where, despite some energy-dependence below the O+C_2H_4 asymptote, the results are relatively independent of energy. The dependence of this branching on the initial rotational state was not considered. Also shown in Fig. 3 are the branching fractions employed by Nguyen et al. [11]. In their model, this branching was controlled by three shallow saddle points connecting the singlet biradical to each of the wells; they did not consider direct branching to the minor channel CH_2CO+H_2 (1f) as suggested elsewhere [8,13]. Agreement between the two (very different) calculations for prompt branching after ISC is again quite remarkable.

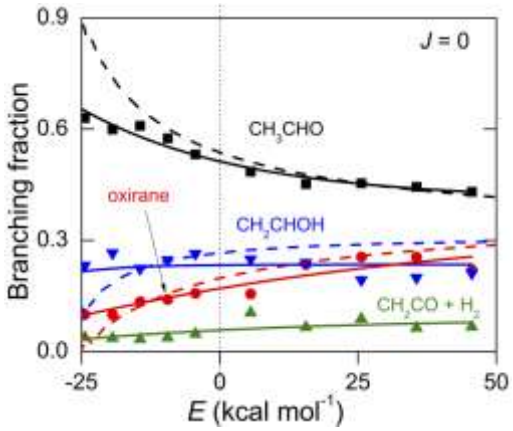

Figure 3: Prompt branching as a function of internal energy *E* for trajectories initiated on the singlet surface with zero angular momentum (*J* = 0) at the MSX (symbols). Solid lines are drawn to fit these results, which show some scatter due to finite sampling statistics. The dashed lines (which do not include the ketene channel) were calculated using the saddle points Nguyen et al. associated with this branching in their ME calculation [11], again for *J* = 0. The zero of energy is the O+C_2H_4 asymptote.

Under conditions relevant to combustion, pressure dependence and stabilization of the intermediates are negligible, as noted above. Instead, the singlet complexes initially produced after ISC decay to bimolecular products, in this case principally to CH_3+HCO (1a).

In Fig. 4, predictions for thermal branching are compared with temperature-dependent experimental results, the room temperature recommendations of Baulch et al. [7], and previous theoretical results [11]. Overall, the agreement of the present results with experiment is excellent at room temperature, with the relatively small theoretically-predicted temperature dependence up to ~600 K largely falling within the experimental error bars. The present theory under-predicts the formation of $^3CH_2$+CH_2O (1e) at 300 K, which is a minor channel at low temperatures. Miyoshi et al. [8] measured 2% branching to CH_2CO+H_2 (1f) at 298 K, which is lower than the present result (4%), while Pruss et al. [37] measured 5%.

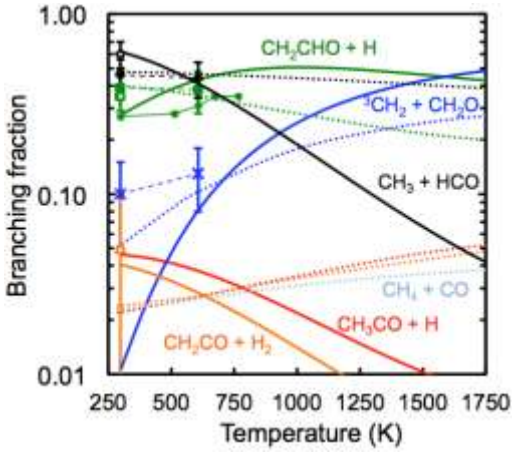

Figure 4: Thermal branching fractions for the present theory (solid lines) and for the theory of Nguyen et al. [11] (dotted lines) compared with two sets of experimental results (closed symbols at 298 and 608 K: Peeters et al. [10]; small green squares up to 770 K: Smalley et al. [9]). Also shown are the recommended room temperature values of Baulch et al. [7] (open symbols).

One source of uncertainty in the present calculations is the magnitude of the spin–orbit coupling, ε. We tested this sensitivity by varying our value (29 cm^{-1}) by 7 cm^{-1}, which corresponds to a ~50% relative change in ε^2 and therefore in the ISC rate. Notably, 22 cm^{-1} is close to the value that would be obtained if only the S_0/T_0 seam were considered, and 36 cm^{-1} is close to value used in some previous surface hopping studies [16,17]. At 1000 K, lowering the ISC rate by 50% resulted in ~10% increases in the rate coefficients for forming CH_2CHO+H (1c) and $^3CH_2$+CH_2O (1e) and a 40% decrease in the formation of CH_3+HCO (1a). Increasing the ISC rate by 50% had the opposite effect. The relative importance of ISC decreases with temperature, and so errors in the ISC rate have a larger impact at lower temperatures than at higher temperatures.

Excellent agreement with the same low-temperature experimental results was found in the previous ME study of Nguyen et al. [11]. The two theories predict very different temperature dependence in the branching fractions, however. Whereas here we predict the CH_2CHO+H (1c) channel to increase somewhat with temperature up to ~750 K and for the CH_3+HCO (1a) and CH_2CHO+H (1c) channels to switch their relative importance around ~600 K, the earlier ME study predicts more CH_3+HCO (1a) than CH_2CHO+H (1c), even up to 2000 K. Both studies show an increase in the importance of CH_2+CH_2O (1e) with temperature, although here this channel becomes important at somewhat lower temperatures. These differences result from the temperature dependence in the overall singlet:triplet branching fraction suggested by Fig. 2 that was included here but not in Ref. [11]. Here, while the singlet:triplet branching fraction is ~50:50 at low temperatures, the relative importance of the triplet species increases with temperature and dominates around 750 K. This may have a notable impact in combustion modeling, which occurs at temperatures above 750 K where no experimental thermal branching information is available. We predict nearly equal amounts of CH_2CHO+H (1c) and CH_2+CH_2O (1e), whereas Nguyen et al. predict significant amounts of the less-reactive products CH_3+HCO (1a).

The present thermal rate coefficients were fit to the following modified Arrhenius expressions, with fitting errors of typically less than 10% for 300–2500 K. Channels 1d (C_2H_3+OH), 1g (CH_4+CO), and 1h (C_2H_2+H_2O) accounted for less than 1% of the products at these conditions and were not fit to modified Arrhenius expressions.

$$k_1 = 1.557 \times 10^{-12} (T/298\ \mathrm{K})^{1.654} \exp(-226.7\ \mathrm{K}/T)\ \mathrm{cm^3\ molecule^{-1}\ s^{-1}}$$
$$k_{1a} = 5.511 \times 10^{-11} (T/298\ \mathrm{K})^{-1.717} \exp(-1456\ \mathrm{K}/T)\ \mathrm{cm^3\ molecule^{-1}\ s^{-1}}$$
$$k_{1b} = 9.108 \times 10^{-13} (T/298\ \mathrm{K})^{-0.4843} \exp(-985.3\ \mathrm{K}/T)\ \mathrm{cm^3\ molecule^{-1}\ s^{-1}}$$
$$k_{1c} = 3.357 \times 10^{-12} (T/298\ \mathrm{K})^{0.9475} \exp(-867.8\ \mathrm{K}/T)\ \mathrm{cm^3\ molecule^{-1}\ s^{-1}}$$
$$k_{1e} = 8.084 \times 10^{-13} (T/298\ \mathrm{K})^{1.991} \exp(-1439\ \mathrm{K}/T)\ \mathrm{cm^3\ molecule^{-1}\ s^{-1}}$$
$$k_{1f} = 5.504 \times 10^{-12} (T/298\ \mathrm{K})^{-1.831} \exp(-1600\ \mathrm{K}/T)\ \mathrm{cm^3\ molecule^{-1}\ s^{-1}}$$

Comparisons were also made with the results of the crossed molecular beam (CMB) studies of Refs. [15,16,17], as shown in Table 1. Overall, the present results are only in fair agreement with the previous measurements, although the discrepancies are sometimes close to the experimental uncertainties. Most notably, the experiments predict very little energy dependence over the two collision energies, whereas the present results vary much more strongly with energy. This can be seen more clearly by considering the total singlet:triplet (S:T) branching ratio, also given in Table 1. Experimentally, this ratio is close to 50:50 and varies only slightly with energy, whereas S:T decreases strongly with energy in the present calculations from 44:56 to 22:78. It is difficult to reconcile a lack of energy dependence in this ratio with the results of Fig. 2, which show a nearly energy independent ISC rate (giving rise to the singlet channels) competing with triplet channel rates that increase sharply with energy. It is possible that effects missing from the Landau-Zener model used here (such as those discussed in Ref. [32]) could lead to a different energy dependence in the ISC rate, although we have no evidence of this for the present system. The results given in the previous master equation study of Nguyen et al. [11], which assumed that the S:T ratio was independent of energy, are in excellent agreement with the higher-energy CMB results.

The results of trajectory surface hopping (TSH) studies that accompanied some of the CMB experiments are also shown in Table 1 [16,17]. In contrast to the present ME results but in agreement

with experiment, these surface hopping results show little energy dependence in S:T over the range of experiments. In an earlier TSH study by a different group [20], the dependence of S:T on the chosen spin–orbit coupling constant was considered. Using ε = 30 cm^{-1}, they obtained S:T = 12:88 at 12.9 kcal/mol, which is in good agreement with our ratio of 22:78 (we used 29 cm^{-1}). They also considered a hyperthermal collision energy (70 kcal/mol) and found S:T to decrease with energy, in agreement with the trends shown here in Fig. 2. They noted better agreement with the CMB experiments at 12.9 kcal/mol using larger values of ε, and the later TSH results of Refs. [16,17] adopted ε = 35 cm^{-1}. Some of the discrepancies among the various theoretical results may then be attributed to different choices for ε, but it is difficult to reconcile the different results based on this choice alone.

Table 1. Product branching fractions (%) at two collision energies

	E_{col} = 8.4 kcal/mol			E_{col} = 12.9 kcal/mol			
Channel	Present	CMB[a]	TSH[a]	Present	CMB[b]	TSH[c]	ME[d]
CH_3+HCO (1a)	37	34 ± 9	49	17	43 ± 11	49	44
CH_3CO + H (1b)	4	3 ± 1	11	2	1 ± 0.5	10	3.5
CH_2CHO+H (1c)	48	30 ± 6	27	55	27 ± 6	28	28
CH_2+CH_2O (1e)	8	20 ± 5	8	23	16 ± 8	8	18
CH_2CO+H_2 (1f)	3	13 ± 4	5	2	13 ± 3	5	3.5
S:T[e]	44:56	50:50	65:35	22:78	57:43	64:36	54:46

[a]Experimental crossed molecular beam (CMB) and theoretical trajectory surface hopping (TSH) results from Ref. [17]. [b]Experimental CMB results from Ref. [15]. [c]Theoretical TSH results from Ref. [16]. [d]The previous ME study of Ref. [11]. [e]Singlet:triplet ratio calculated by assigning 1c and 1e as triplet channels and 1a, 1b, and 1f as singlet channels.

4. Conclusions

An ab initio transition state theory based master equation approach was used to predict the kinetics of ^3O+C_2H_4, including an a priori description of ISC. The present results are in good agreement with existing experimental thermal kinetics and largely with past theoretical work, including the earlier comprehensive ME study of Nguyen et al. [11]. Notably, however, the present and earlier ME studies differ in their predicted product branching fractions at elevated temperature due to their different treatments of ISC. At elevated temperatures, we predict CH_2CHO+H and CH_2+CH_2O exclusively as the

major products, which differs from the room temperature preference for CH_3+HCO and from the results of Ref. [11].

Acknowledgments

This work is supported by the Division of Chemical Sciences, Geosciences, and Biosciences, Office of Basic Energy Sciences, U.S. Department of Energy. Sandia is a multiprogram laboratory operated by Sandia Corporation, a Lockheed Martin Company, for the United States Department of Energy under Contract No. DE-AC04-94-AL85000. The work at Argonne was supported under Contract No. DE-AC02-06CH11357. Software development was supported by the AITSTME project as part of the Predictive Theory and Modeling component of the Materials Genome Initiative.

References

[1] C.P. Fenimore, Proc. Comb. Inst. 13 (1971) 373–80.

[2] J.A. Miller, and C.T. Bowman Prog. Energy Combust. Sci. 15 (1989) 287–338.

[3] J.A. Miller, M.J. Pilling, and J. Troe, Proc. Comb. Inst. 30 (2005) 43–88.

[4] L.B. Harding, S.J. Klippenstein, J.A. Miller, J. Phys. Chem. A 112 (2008) 522–532.

[5] L.V. Moskaleva and M.C. Lin, Proc. Comb. Inst. 28 (2000) 2393–2401.

[6] R.J. Cvetanović, J. Phys. Chem. Ref. Data 16 (1987) 261–326.

[7] D.L. Baulch, C.T. Bowman, C.J. Cobos, R.A. Cox, T. Just, J.A. Kerr, M.J. Pilling, D. Stocker, J. Troe, W. Tsang, R.W. Walker, and J. Warnatz, J. Phys. Chem. Ref. Data 34 (2005) 757–1397.

[8] A. Miyoshi, J.-I. Yoshida, N. Shiki, M. Koshi, and H. Matsui, Phys. Chem. Chem. Phys. 11 (2009) 7318–7323.

[9] J.F. Smalley, F.L. Nesbitt, R.B. Klemm, J. Phys. Chem. 90 (1986) 491.

[10] J. Peeters, D. Maes, Tenth Int. Symp. Gas Kinetics, University College of Swansea, July 1988, p. A31.

[11] T.L. Nguyen, L. Vereecken, X.J. Hou, M.T. Nguyen, and J. Peeters, J. Phys. Chem. A, 109 (2005) 7489.

[12] U. Bley, P. Dransfeld, B. Himme, M. Koch, F. Temps, and H. G. Wagner, Proc. Combust. Inst. 22 (1998) 997.

[13] A.M. Schmoltner, P.M. Chu, R.J. Brudzynski, and Y.T. Lee, J. Chem. Phys. 91 (1989) 6926.

[14] M.L. Morton, D.E. Szpunar, and L.J. Butler, J. Chem. Phys. 115 (2001) 204.

[15] P. Casavecchia, G. Capozza, E. Segoloni, E. Segologi, F. Leonori, N. Balucani, and G.G. Volpi, J. Phys. Chem. A 109 (2005) 3527.

[16] B. Fu, Y.-C. Han, J. M. Bowman, F. Leonori, N. Balucani, L. Angelucci, A. Occhiogrosso, R. Petrucci, and P. Casavecchia, J. Chem. Phys. 138 (2012) 22A532.

[17] N. Balucani, F. Leonori, P. Casavecchia, B. Fu, and J. M. Bowman, J. Phys. Chem. A, 50 (2015) 12498–12511.

[18] J.C. Tully, J. Chem. Phys. 93 (1990) 1061.

[19] A.W. Jasper, C. Zhu, S. Nangia, and D.G. Truhlar, Faraday Discuss. 127 (2004) 1–22.

[20] W. Hu, G. Lendvay, B. Maiti, and G.C. Schatz, J. Phys. Chem. A 112 (2008) 2093–2103.

[21] M.M. Kopp, E.L. Petersen, W.K. Metcalfe, S.M. Burke, and H.J. Curran, J. Propul. Power 30 (2014) 799-811.

[22] M.M. Kopp, N.S. Donato, E.L. Petersen, W.K. Metcalfe, S.M. Burke, and H.J. Curran, J. Propul. Power 30 (2014) 790-798.

[23] A.C. West, J.D. Lynch, B. Sellner, H. Lischka, W.L. Hase, and T.L. Windus, Theor. Chem. Acc. 131 (2012) 1123.

[24] J.M.L. Martin, O. Uzan, Chem. Phys. Lett. 282 (1998)16-24.

[25] D.E. Woon, T.H. Dunning, J. Chem. Phys. 103 (1995) 4572-4585.

[26] MRCC, a string-based quantum chemical program suite; written by M. Kállay, see also M. Kállay, P.R. Surján, Higher Excitations in Coupled-Cluster Theory. J. Chem. Phys. 115, (2001) 2945-2954.

[27] S.J. Klippenstein, L.B. Harding, B. Ruscic, Ab initio computations and active thermochemical tables hand in hand: Heats of formation of core combustion species, manuscript in preparation (2015).

[28] Y. Georgievskii, S.J. Klippenstein, J. Phys. Chem. A 107 (2003) 9776-9781

[29] L.B. Harding, Y. Georgievskii, S.J. Klippenstein, J. Phys. Chem. A, 114 (2010) 765-777.

[30] Q. Cui, K. Morokuma, J.M. Bowman, and S.J. Klippenstein, J. Chem. Phys. 110 (1999) 9469.

[31] J.N. Harvey, Phys. Chem. Chem. Phys. 9 (2007) 331.

[32] A.W. Jasper, J. Phys. Chem. A 119 (2015) 7339.

[33] C. Angeli, R. Cimiraglia, and J.-P. Malrieu, J. Chem. Phys. 117 (2002) 9138.

[34] F. Neese, WIREs: Comp. Mol. Sci. 2 (2012) 73.

[35] Y. Georgievskii, S.J. Klippenstein, Master Equation System Solver (MESS), 2015, online at http://tcg.cse.anl.gov/papr.

[36] Y. Georgievskii, J.A. Miller, M.P. Burke, S.J. Klippenstein, J. Phys. Chem. A 117 (2013) 12146-12154.

[37] F.J. Pruss, Jr., I.R. Slagle, and D. Gutman, J. Phys. Chem. 78 (1974) 663.

Figure Captions

Figure 1: Potential energy diagrams for the (A) triplet and (B) singlet channels. The MSX promoting ISC is close to the triplet biradical $^3CH_2CH_2O$, and the immediate products formed after ISC are indicated by arrows in B.

Figure 2: Unimolecular transition state theory rate coefficients (k_{TST}) for the fate of the triplet adduct $^3CH_2CH_2O$. The zero of energy is the $O+C_2H_4$ asymptote.

Figure 3: Prompt branching for trajectories initiated on the singlet surface at the MSX as a function of internal energy (symbols). Solid lines are drawn to fit these results, which show some scatter due to incomplete statistics. The dashed lines (which do not include the ketene channel) were calculated using the saddle points Nguyen et al. associated with this branching in their ME calculation [11]. The zero of energy is the $O+C_2H_4$ asymptote.

Figure 4: Thermal branching fractions for the present theory (solid lines) and for the theory of Nguyen et al. [11] (dotted lines) compared with two sets of experimental results (closed symbols at 298 and 608 K: Peeters et al. [10]; small green squares up to 770 K: Smalley et al. [9]). Also shown are the recommended room temperature values of Baulch et al. [7] (open symbols).